Catalysis Today xxx (xxxx) xxx–xxx

Contents lists available at ScienceDirect

Catalysis Today

journal homepage: www.elsevier.com/locate/cattod

# First-principle investigation on catalytic hydrogenation of benzaldehyde over Pt-group metals

Simuck F. Yuk[a,1], Mal-Soon Lee[a,*], Sneha A. Akhade[a,b], Manh-Thuong Nguyen[a], Vassiliki-Alexandra Glezakou[a], Roger Rousseau[a]

[a] Basic & Applied Molecular Foundations, Physical and Computational Sciences Directorate, Pacific Northwest National Laboratory, Richland, WA 99352, USA
[b] Material Sciences Division, Lawrence Livermore National Laboratory, Livermore, CA 94550, USA

ARTICLE INFO

*Keywords:*
Hydrogen adsorption
Catalytic hydrogenation
Metal catalyst
Solid/liquid interface
Ab initio molecular dynamics

ABSTRACT

Understanding the hydrogenation of organic compounds in the aqueous phase has always been fundamentally important for improving carbon neutral pathways to fuels and value-added chemicals. In this study, we investigated both thermodynamic and kinetic profiles of benzaldehyde hydrogenation over the Pd(111) and Pt (111) metal surfaces using density functional theory (DFT) and *ab initio* molecular dynamic (AIMD) simulations. The adsorption of $H_2$ shows the mixed preference of H adsorption sites on the Pt(111), while the fcc adsorption site is dominant for H on the Pd(111). When benzaldehyde is added to the systems, we observe a strong reduction of benzaldehyde on charged Pd (111) surface compared with that on neutral surface. In contrast, charged state of the Pt(111) surface does not change their interaction. Subsequent hydrogenation reaction of benzaldehyde over Pd(111), proceeding via Langmuir-Hinshelwood mechanism, is affected by two major factors: the presence of $H_2O$ solvent and surface charge. The presence of $H_2O$ solvent greatly reduces the activation energy of C—H and O—H bond formation during the hydrogenation process. Furthermore, the hydrogenation step via C—H bond formation is preferred thermodynamically and kinetically over O—H bond formation during thermocatalytic hydrogenation, while the opposite trend holds true during electrocatalytic hydrogenation.

## 1. Introduction

There have been increasing efforts in using biomass for energy applications to displace or supplement petroleum-based fuels and chemicals [1–3]. This has been attributed in part to an increasing need in today's energy economy to efficiently produce fuels and chemicals, meet expanding fuel demands in heavy duty transportation while simultaneously eliminating carbon & environmental footprints. To develop sustainable fuels and chemicals, the effective H/C ratio of these organic feedstocks (for instance, biomass or $CO_2$) must be increased up to 2, the average value required for transportation fuels [4]. Hydrogen addition can increase the H/C ratio without loss of carbon. The efficacy of the entire process to generate desirable fuels and chemicals is entirely reliant on having active, stable and efficient catalyst materials.

Catalytic hydrogenation reactions of organic compounds over metal surfaces is of high relevance in catalysis science [3,5–9]. Considerable research efforts have been made to explore both gaseous- and solution-phase thermal catalytic hydrogenation (TCH) and aqueous-phase electrocatalytic hydrogenation (ECH) of organic compounds in gas and aqueous phases [7–20]. One of the suggested mechanisms for hydrogenation process, termed "Langmuir Hinshelwood" (LH) scheme [14,21], comprises of a two-step process that involves the dissociative adsorption of hydrogen ($H_2 \rightarrow 2H^*$) to the metal surface and subsequent transfer of the surface-bound hydrogen to the adsorbed organic species. Benzene hydrogenation over Pt catalysts supported on various oxide substrates was shown to proceed via such a LH mechanism under TCH [10]. Other reports suggested that the mechanism for phenol hydrogenation over Pt and Ni catalysts under reducing conditions also proceeds via a LH scheme [14]. A recent study comparing the reaction rates of thermal and electrochemical hydrogenation of benzaldehyde on carbon supported Pt-group metals confirmed similar reaction orders of hydrogen and organics, which suggests that the hydrogenation can follow a similar type of mechanism at least at lower applied voltages [8,18]. Likewise, ECH of phenol over $Pd/Al_2O_3$ is also postulated to proceed via a LH-like mechanism [13].

In all these cases, the basis for efficient conversion of benzaldehyde to benzyl alcohol is intrinsically linked to the availability of hydrogen on the metal surface and the mechanism of hydrogen addition. Detailed

* Corresponding author.
*E-mail address:* malsoon.lee@pnnl.gov (M.-S. Lee).
[1] Current address: Department of Chemistry and Life Science, United States Military Academy, West Point, NY 10996, USA.

https://doi.org/10.1016/j.cattod.2020.07.039
Received 11 March 2020; Received in revised form 15 June 2020; Accepted 20 July 2020

information on the environment driven mechanism of hydrogen adsorption and transfer at the metal surface, however, is generally lacking particularly in the presence of solvent and charge. Such information is mandatory for a knowledge-based development of thermal or electrocatalysis, to achieve high activity and selectivity during the conversion process. Few recent studies have attempted to address these unknowns. Numerous first-principles studies have also explored the adsorption profile of $H_2$ in gas phase over various types of metal surfaces, showing the distribution of $H_2$ adsorption over the fcc (face centered cubic), hcp (hexagonal close packed), bridge, and top sites [22–26]. Although these studies exclude solvent effects, they all highlight the susceptibility of hydrogen adsorption to the metal facet and active site. Yang et al. have recently reported that the surface H coverage over Pt(111) is significantly higher in the gas phase relative to the presence of $H_2O$ solvent which is due to both enthalpic and entropic drivers that significantly decrease the free energy of $H_2$ adsorption [27]. Ultimately, lower surface coverage will result in lower rates in a LH mechanism.

Therefore, we must start by addressing the largest identified gap – the lack of qualitative and quantitative information on how metal surfaces act as effective sources or sinks for hydrogen that participate in electrocatalyzed reactions. Several challenges exist in closing this gap: (a) The extent of hydrogen that gets adsorbed and desorbed at the metal surface is strongly influenced and controlled by the environment. The liquid phase environment alters the dynamics and chemical interaction between the metal and hydrogen and introduces complexity to developing an in-situ, operando understanding of the electrocatalytic reduction mechanism [17,18,27]. (b) In situ operando experiments are difficult and require high precision. Spectroscopic characterization of hydrogenation phenomena is non-trivial, requires high-precision and entails probing of the surface under real-time operating conditions [8,27].

In this study, we address these information gaps using first-principles simulations of the solvated metal surface. The nature and role of surface bound hydrogen in reducing benzaldehyde on Pt and Pd surfaces are investigated under neutral (open-circuit potential) and charged (reducing) conditions. We postulate that the presence of surface-bound H atoms on the metal surfaces is critical for driving the hydrogenation reaction. Using density functional theory calculations and ab initio molecular dynamics simulations, the adsorption features, site distribution and surface H coverage on Pd(111) and Pt(111) surfaces are compared and found to be distinct. The adsorption geometry of benzaldehyde on the H-covered Pd(111) and Pt(111) surfaces is compared under TCH and ECH conditions. Lastly, both thermodynamic and kinetic profiles of benzaldehyde hydrogenation to benzyl alcohol are investigated on the Pd(111) based on a LH mechanism. We show that the reaction pathways of benzaldehyde hydrogenation are significantly affected by the consideration of $H_2O$ solvent and surface charge.

## 2. Computational methodology

We performed periodic density functional theory (DFT) calculations using the Perdew, Burke, and Ernzerhof (PBE) [28] form of the generalized gradient approximation (GGA), as implemented in the CP2K software package [29,30]. The norm-conserving pseudopotentials [31] were employed to describe the core electrons, while the valence wave functions were expanded in the form of double-ζ-quality Gaussian basis sets optimized for condensed phase systems [32]. A 400 Ry cutoff was chosen to compute the electrostatic terms. The Γ-point approximation was used for integrating the Brillouin zone. Long-range dispersion (van der Waals) interactions were treated through Grimme's DFT-D3 approach [33].

Pd(111) and Pt(111) slabs, consisting of 192 Pd/Pt atoms (48 atoms/layer), were constructed with cell dimensions of 18.86 × 16.33 × 26.67 Å and 19.18 × 16.61 × 26.78 Å, respectively, with 20 Å vacuum space. The (111) facet is chosen over the (100) and (110) facets due to its relative stability for both Pd and Pt surfaces [34–36]. Singh et al. also showed that Pd(111) is the most active surface for benzaldehyde hydrogenation [8]. Two different types of configurations were used to explore the effects of solvents on the $H_2$ adsorption and hydrogenation of benzaldehyde on Pd and Pt surfaces: 1) with 25 $H_2$ molecules on the surface (representing a gas-phase system) and 2) with 25 $H_2$ and 139/144 $H_2O$ molecules on the Pd/Pt surface (representing a solvent system). The number of water molecules was chosen to reflect a bulk water density of ~1.0 gm/cm$^3$ with a $H_2$ partial pressure ($p_{H_2}$) of 6700 bar, as estimated from Henry's law constant. We choose this high pressure of $H_2$ to accelerate adsorption/desorption process from the surface to more rapidly converge the AIMD simulations on picosecond time scale [27]. After thermal equilibration of systems, we further added one benzaldehyde on Pd(111) and Pt(111) surface to investigate the hydrogenation of benzaldehyde to benzyl alcohol. In addition, for a charged surface, incorporation of one extra electron into the simulation cell imparts a surface charge of ~0.01 electron/Pd surface atom (0.3 e-/nm$^2$, approximately 0.8 V applied potential).

The DFT-based *ab initio* molecular dynamics (AIMD) simulations were performed within the canonical NVT ensembles, using a 1 fs time step and a Nosé-Hoover chain thermostat at 373 K. Simulations of 10–15 ps were carried out after equilibration in order to obtain reliable statistics and a dynamic distribution of solvent molecules. Simulated annealing of post-MD structures was subsequently performed in order to obtain the most stable structure of surface-bound states. The obtained structure was used to investigate electronic structural properties and interfacial interactions such as binding energy of hydrogen and/or benzaldehyde. In addition, the reaction mechanism of benzaldehyde hydrogenation on Pd(111) surface was explored using the climbing-image nudged elastic band (CI-NEB) method [37]. We relaxed the configurations in the CI-NEB by a MD-simulated annealing to allow the $H_2O$ structure to adiabatically relax about the reaction coordinate to remove artifact resulting from metastable solvent configurations [14].

## 3. Results and discussions

### 3.1. Hydrogen on solvated Pt(111) and Pd(111) surfaces

Fig. 1 shows atomic density profiles (in molecules/Å$^3$) of H (adsorbed and molecular), O of $H_2O$, and Pd/Pt atoms as a function of the

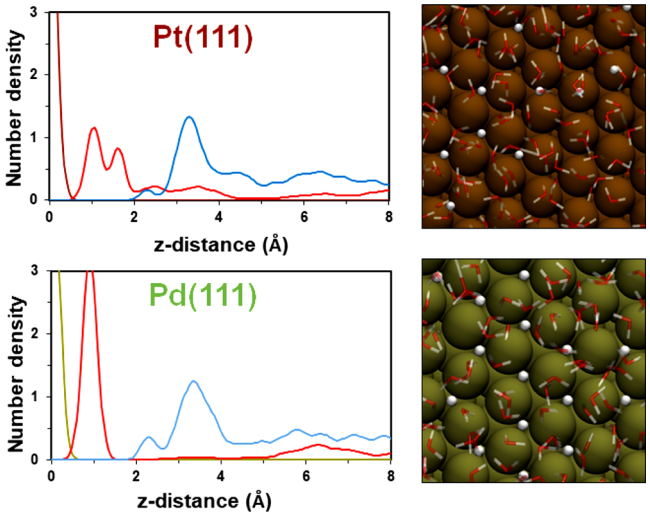


**Fig. 1.** Atomic density profile of H, O of $H_2O$, and surface Pt/Pd atom on the neutral surface as a function of the surface normal (z) direction in the presence of $H_2O$ solvent. Color codes for density profiles: H (red line), O of $H_2O$ (blue line), Pt (brown line), and Pd (tan line). Color codes for surface models: H (white), O (red), Pt (brown) and Pd (tan). (For interpretation of the references to colour in the Figure, the reader is referred to the web version of this article).

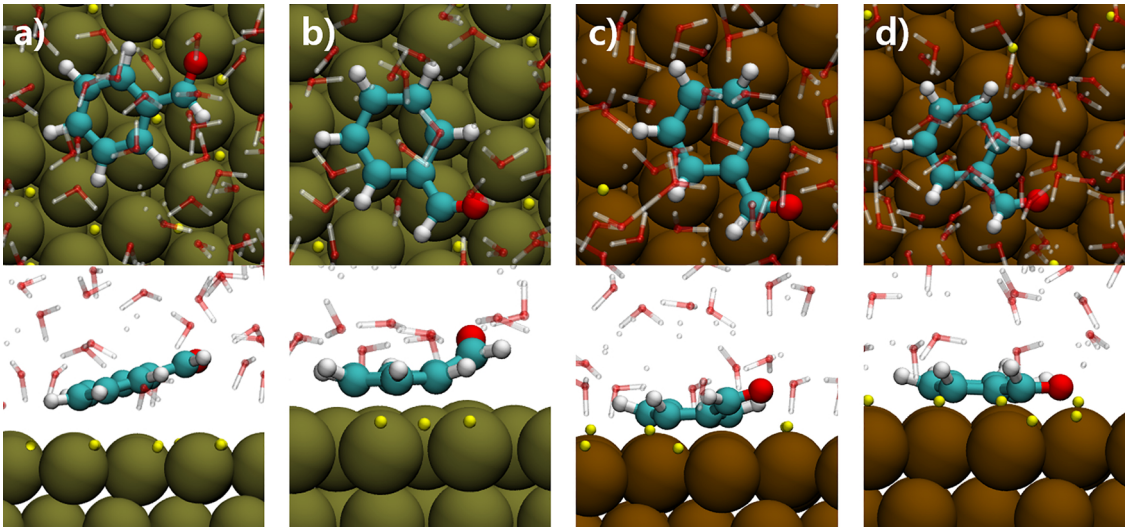


**Fig. 2.** DFT-optimized geometry of adsorbed benzaldehyde on a) neutral and b) charged Pd(111) surface in comparison to adsorbed benzaldehyde on c) neutral and d) charged Pt(111) surface in the presence of $H_2O$ solvent. Color codes for surface models: C (cyan), H (white), surface-bound H (yellow), O (red), Pt (orange) and Pd (tan). (For interpretation of the references to colour in the Figure, the reader is referred to the web version of this article).

surface normal (z) direction calculated from equilibrated MD trajectories, which illustrates the distributions of species along z-direction. A double peak associated with H (red peak) can be seen in the range of 0 to 2 Å for the Pt(111), indicating the mixture of H adsorption sites on the Pt surface. Structural visualization with VMD [38] reveals that the first higher peak from the surface is due to H adsorption on hollow sites (fcc or hcp) while the second lower peak is associated with atop adsorption of H. Adsorbed H freely diffuses on the surface and interchanges between atop and hollow sites on the picosecond time scale. Interestingly, our simulation shows opposite intensity of these distribution in the gas phase system (see Figure S1 of Supporting Information (SI)), but diffusion and interchange of sites persist. Given the rapid interchange of positions, we can assume that the MD is equilibrated and the observed populations reflect the relative free energetics of the binding sites, $\Delta G_{site} = RTln(\frac{P_{atop}}{P_{hollow}})$, with $p_j$ representing the population of sites occupied by H atom. Therefore, solvent is perturbing relative free energy of binding sites such that at 373 K, atop sites are preferred over hollow sites by ~2 kJ/mol in the gas phase whereas hollow sites are preferred by ~2 kJ/mol in the presence of $H_2O$. In contrast, only one sharp peak associated with H bound at hollow site (mostly fcc) is observed on the Pd(111) surface for both gas and aqueous phases.

In addition, a broad peak associated with freely diffusing $H_2$ molecules in the solvent can be seen above 2 Å for Pt(111), while such peak is shifted to above 8 Å on Pd(111). The distribution peak of $H_2O$ (blue peak) is also different between Pt(111) and Pd(111) surfaces. The peak at ~2 to 4 Å is 50 % higher on Pd relative to Pt, indicating that the first $H_2O$ layer is more ordered with a tighter packing of $H_2O$ molecules. This higher density of $H_2O$ in the first layer excludes freely diffusing $H_2$, leading to the shifting of freely diffusing $H_2$ peak to above 8 Å on Pd (111) and indicates a kinetic barrier for $H_2$ adsorption/desorption. Note however, no exchange of adsorbed H to the $H_2O$ solvent is observed on either surface within the time frame of the current AIMD simulations.

On the other hand, the total amount of surface-bound H presented on Pd surface (~0.6 monolayer (ML) of H) is almost twice as much compared to the Pt surface (~0.3 ML of H). Such site distribution and coverage of surface-bound H shows that the surface H coverage is clearly affected by the underlying metal surface. This difference in coverage can be understood in very simple terms. From our previous work [27], we know that $H_2O$ has two effects on H binding at surfaces: 1) reduction of the enthalpy of binding due to the lowering of the work function of the metal as a consequence of presence of $H_2O$ at the surface and 2) increased entropic contribution due to $H_2O$ restructuring and hindered H diffusion. Assuming that the entropic contribution is approximately similar between the surfaces and noting that the expected shift in work function is also similar between the surfaces [14], the difference should strictly be related to the relative binding energy of H between the two surfaces. We computed that $\Delta H_{ads}$ of $H_2$ on Pd(111) is ~15.0 kJ/mol lower than on Pt(111), consisted with previous theoretical studies [26,39,40]. Theoretically, $\Delta G^o_{ads}$ of $H_2$ for Pt(111) is found to be ~ −1.0 kJ/mol [27], which can serve as a basis to estimate $\Delta G^o_{ads}$ of $H_2$ observed for Pd(111). Under the above assumptions, $\Delta G^o_{ads}$ of $H_2$ for Pd(111) equals the addition of $\Delta G^o_{ads}$ of $H_2$ for Pt(111) and $\Delta\Delta H^o_{ads}$ of $H_2$, which is ~ −16.0 kJ/mol. Using LH isotherm estimates of coverage [41], we conclude that at 343 K and 1 bar of $H_2$, the surface coverage of Pt would be ~0.5, whereas Pd would be ~0.9. Note that in both cases, the coverage of H is appreciably lower than in the gas phase at the same thermodynamic conditions where the H coverage is expected to be unity.

It should be noted that the formation of beta hydride is experimentally shown to be suppressed in the presence of benzaldehyde and only observable under elevated hydrogen pressure. Likewise, our simulation observed the formation of subsurface H atoms only in the presence of a very large number $H_2$ molecules (see Fig. S2 of SI). These results suggest that the hydride formation is thermodynamically difficult to access in this reaction condition and, therefore, we focus solely on reactivity with surface-bound H in our study.

### 3.2. Adsorption of benzaldehyde on (111) surfaces

The DFT-optimized geometry of various organic compounds, including benzaldehyde and phenol, has been reported on (111) surfaces where the benzene ring lies flat with the functional group being titled away from the surface [14,42–45]. Thus, a similar adsorption geometry of benzaldehyde was adopted and further refined over H-covered Pd (111) and Pt (111) surfaces using the DFT and AIMD simulations. The DFT-optimized structures, resulting from AIMD followed by simulated annealing, of adsorbed benzaldehyde on H-covered (111) surfaces are summarized in Fig. 2. Two important factors were incorporated when calculating the adsorption geometry of benzaldehyde on the Pd and Pt surfaces: 1) $H_2O$ solvent, which is present under thermo and electrochemical conditions and expected to also reduce the binding of the organics [46,47] and 2) surface charge, which is present under electrochemical condition and also impacts organic binding [18,19].

It is interesting to note that the adsorbed benzaldehyde moves away from neutral Pd(111) surface (see Fig. 2a) relative to the gas phase configuration. For instance, the mean Pd-C separation distance in gas phase is ~2.2 Å whereas such distance increase to ~3.2 Å angstroms in the presence of $H_2O$. Incorporation of one extra electron into the simulation cell imparts a surface charge of ~0.01 electron/Pd surface atom (0.3 e-/nm$^2$, approximately 0.8 V applied potential) yet has a profound impact on binding of benzaldehyde. The mean Pd-C separation distance decreases to ~2.2 Å and now the benzene ring of adsorbed benzaldehyde is parallel to the Pd surface whilst the carbonyl group is titled away (see Fig. 2b). Such drastic change in adsorption geometry of benzaldehyde is not seen on Pt(111) where adsorbed benzaldehyde lies parallel to both neutral and charged Pt surfaces (see Fig. 2c and d). Furthermore, the adsorption of benzaldehyde on Pt surface shows an increased Pt-C distance of 2.28 Å on charged surface compared to that of 2.07 Å on neutral surface. These results indicate a weakened adsorption of benzaldehyde on charged surface, which is also consistent with the values reported by Bockris and Jeng [48].

To further understand the adsorption feature of benzaldehyde on Pd (111), we further calculated the charge differential profile of all chemical species presented on the surface and the distribution of surface species projected on the z axis averaged over the MD trajectories, as shown in Fig. 3. The density distribution of surface-bound H as well as $H_2$ molecule on the surface is not significantly affected by the presence of surface charge on Pd(111). Note comparing the freely diffusing $H_2$ density on Pt surface (Fig. 1b), there is an increase in $H_2$ closer to the surface in the presence of benzaldehyde (see Fig. 3a), indicating that benzaldehyde has broken up the surface $H_2O$ layer, which inhibited the access of $H_2$ to the surface. In contrast, no significant change in atomic density profile of adsorbed H or benzaldehyde is seen on Pt(111) (see Figure S3 of SI for details). As already described in Fig. 2a and b, we also observed that both the benzene ring and carbonyl group move closer to the charged Pd surface (see Fig. 3b) compared to the neutral Pd surface (see Fig. 3a). The origin of this drastic change can be understood from the differential charge density profiles which show a clear charge transfer between adsorbed benzaldehyde and the charged Pd surface (see Fig. 3b). Such phenomenon is completely absent for the Pd neutral surface (see Fig. 3a). This can be understood by the fact that the LUMO of benzaldehyde is approximately 1.0 eV above the Fermi level of neutral Pd and the addition of charge shifts the work function by 0.8 eV, leading to the partial charge transfer to the organic. This suggests that at applied voltage in the range of 0.8 eV or higher, a proton-coupled electron transfer type mechanism may also be possible [7,9,49]. The calculated potentials relative to relative to standard hydrogen electrode (SHE) and reversible hydrogen electrode (RHE) scale are also summarized in Table S1 of SI for neutral and charged Pd and Pt (111).

We also investigated whether the site distribution of surface-bound H is affected by the adsorption of benzaldehyde. Again, density profiles of surface-bound H atoms were calculated over the neutral and charged Pt and Pd surfaces, seen in Fig. 4. A clear difference is seen for the site distribution of surface-bound H between neutral and charged Pt surfaces even without the presence of adsorbed benzaldehyde (see Fig. 4a). The disappearance of sharp peak just below 2 Å indicates that the surface-bound H migrates towards one particular type of site as surface charge is introduced to Pt(111). Note there is a finite density above 2 Å for both charged and neutral surfaces owing to $H_2$/H interchange with the bulk even at the MD time scale, indicative of the fact that HER is

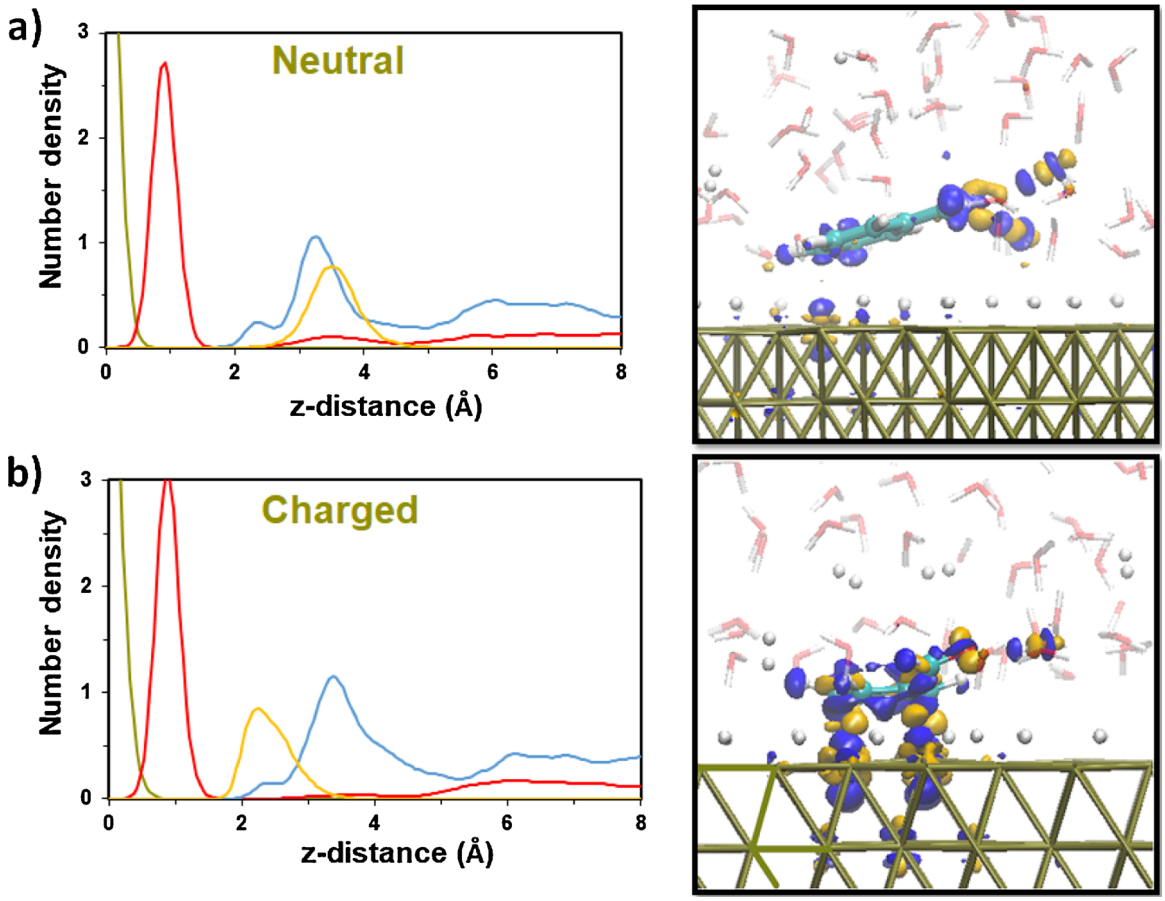


**Fig. 3.** Atomic density profile and differential charge profile of adsorbed benzaldehyde, along with surface-bound H atoms and $H_2$ molecules on a) neutral and b) charged Pd(111). Color codes for density profiles: H (red line), O of $H_2O$ (blue line), C of benzaldehyde (yellow line), and Pd (tan line). Color codes for surface models: H (white), O (red), C (cyan) and Pd (tan). (For interpretation of the references to colour in the Figure, the reader is referred to the web version of this article).

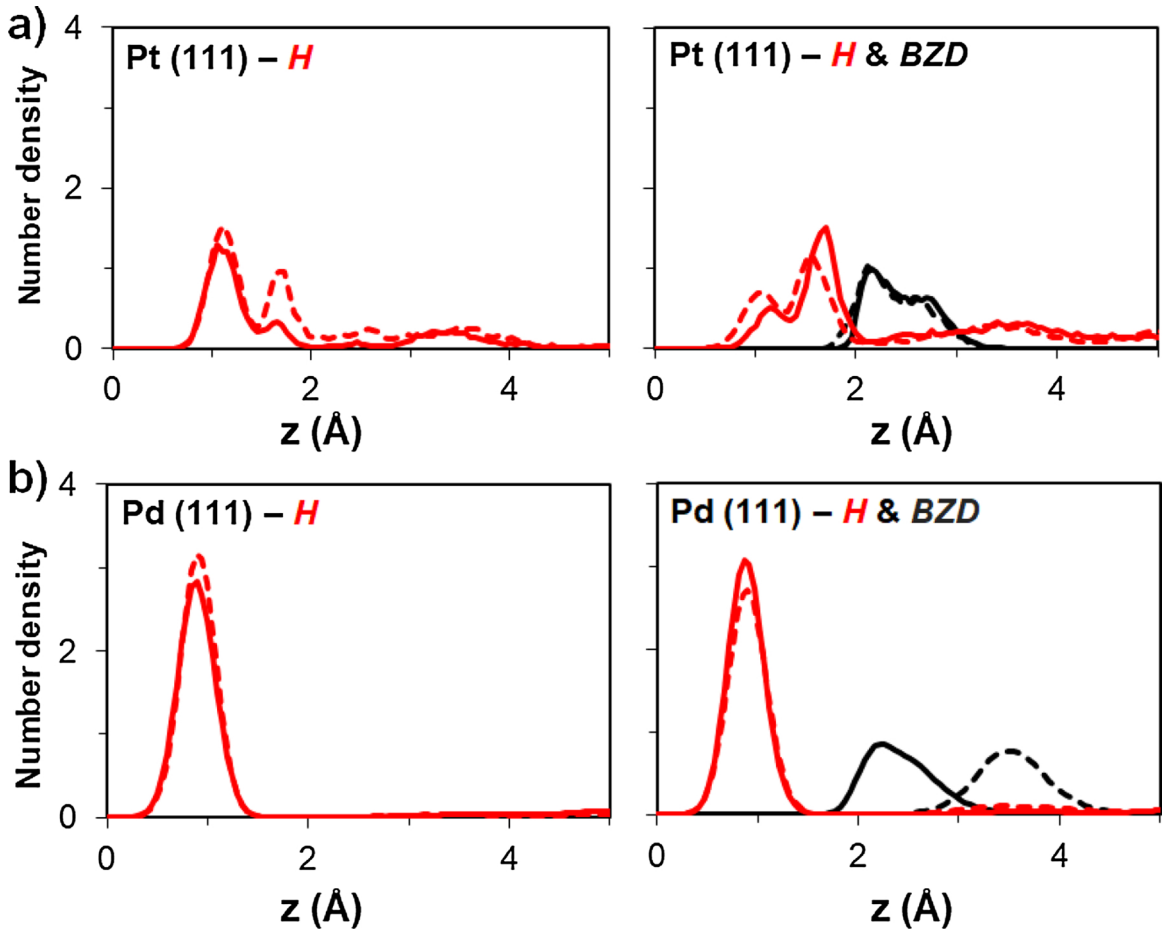


**Fig. 4.** Atomic density profile of surface-bound H and benzaldehyde over neutral and charged a) Pt and b) Pd(111) surfaces. Note that dotted lines represent the neutral surface (0.0 e-/nm$^2$), while solid lines represent the charged surface (0.3 e-/nm$^2$).

likely to occur on the Pt surface even at the lower applied potential. The density profile becomes greatly changed for surface-bound H in the presence of adsorbed benzaldehyde, signifying there is a site competition between adsorbed H and benzaldehyde on the Pt(111) (see Fig. 4a) as also observed by EXAFS [18]. In contrast, there are only slight changes seen with the surface-bound H on both neutral and charged Pd (111) (see Fig. 4b). The adsorption of benzaldehyde also doesn't induce any change in the density profile feature, showing that the surface-bound H atoms are largely unaffected with the introduction of adsorbed benzaldehyde onto the Pd(111). Lastly, when comparing Pd(111) with Pt(111), there is appreciably less interchange between H on the surface and solvated $H_2$ on Pd(111), which is consistent with the lower efficiency of Pd as an HER catalyst. Note that this enables HER and ECH to be more competitive on Pd than Pt where the former is strongly preferred [18].

### 3.3. Benzaldehyde hydrogenation over Pd(111)

In this section, we will now consider the factors influencing the rate of a LH hydrogenation mechanism. Now, we investigated the hydrogenation reaction of benzaldehyde to benzyl alcohol over Pd(111) surface. Pd is chosen for this study due to its outstanding intrinsic rates of ECH of benzaldehyde compared to other Pt-group metals [19]. As mentioned, depending on the reaction conditions, we consider that benzaldehyde hydrogenation is proceed via Langmuir-Hinshelwood mechanism where the addition of surface-adsorbed H atom to the adsorbed benzaldehyde leads to the formation of benzyl alcohol. We can write the rate, $r_{LH}$, as [19]:

$$r_{LH} = k \bullet \theta_{BEN} \bullet \theta_H = \frac{k \bullet K_{BEN} \bullet [BEN] \bullet K_{Volmer} \bullet [H_3O^+]}{(1 + K_{BEN} \bullet [BEN] + K_{Volmer} \bullet [H_3O^+])^2}$$

where $\theta_H$ and $\theta_{BEN}$ are the coverage of H and benzaldehyde (BEN), respectively. $k$ represents the effective rate constant, while $K_j$ defines the adsorption equilibrium constant of benzaldehyde or H. [j] is the concentration of benzaldehyde or hydronium ions ($H_3O^+$). Given the discussion above, it is clear that Pd will have a higher H coverage than Pt under all circumstances and is thus expected to exhibit a higher rate [8,19]. Hence, the following discussion will focus predominantly on Pd (111), but as will be apparent the results are also applicable to metal surfaces in general.

We now consider factors which influences $k$, the effective rate constant. Specifically, either the C or O atom of carbonyl group (−CHO) can first be hydrogenated with the surface-adsorbed H atom, resulting in two distinctive pathways (C−H vs. O−H bond formation) for hydrogenation reaction. The energy difference between C−H and O−H bond formation routes is already seen with $CO_2$ reduction process over transition metals [50]. Thus, the DFT-based C−H and O-H reaction pathways of benzaldehyde hydrogenation are computed over the Pd (111) with and without the presence of $H_2O$ solvent and surface charge, as summarized in Fig. 5.

Without the presence of $H_2O$ solvent (see Fig. 5b), it is thermodynamically preferable for benzaldehyde hydrogenation to be proceed through the O-H pathway over neutral Pd surface since the reaction intermediate of the O−H pathway is thermodynamically downhill, unlike that of the C−H pathway. From kinetic perspective, while the O−H pathway has a lower activation barrier compared to the C−H pathway for the first hydrogenation step, the opposite trend holds true

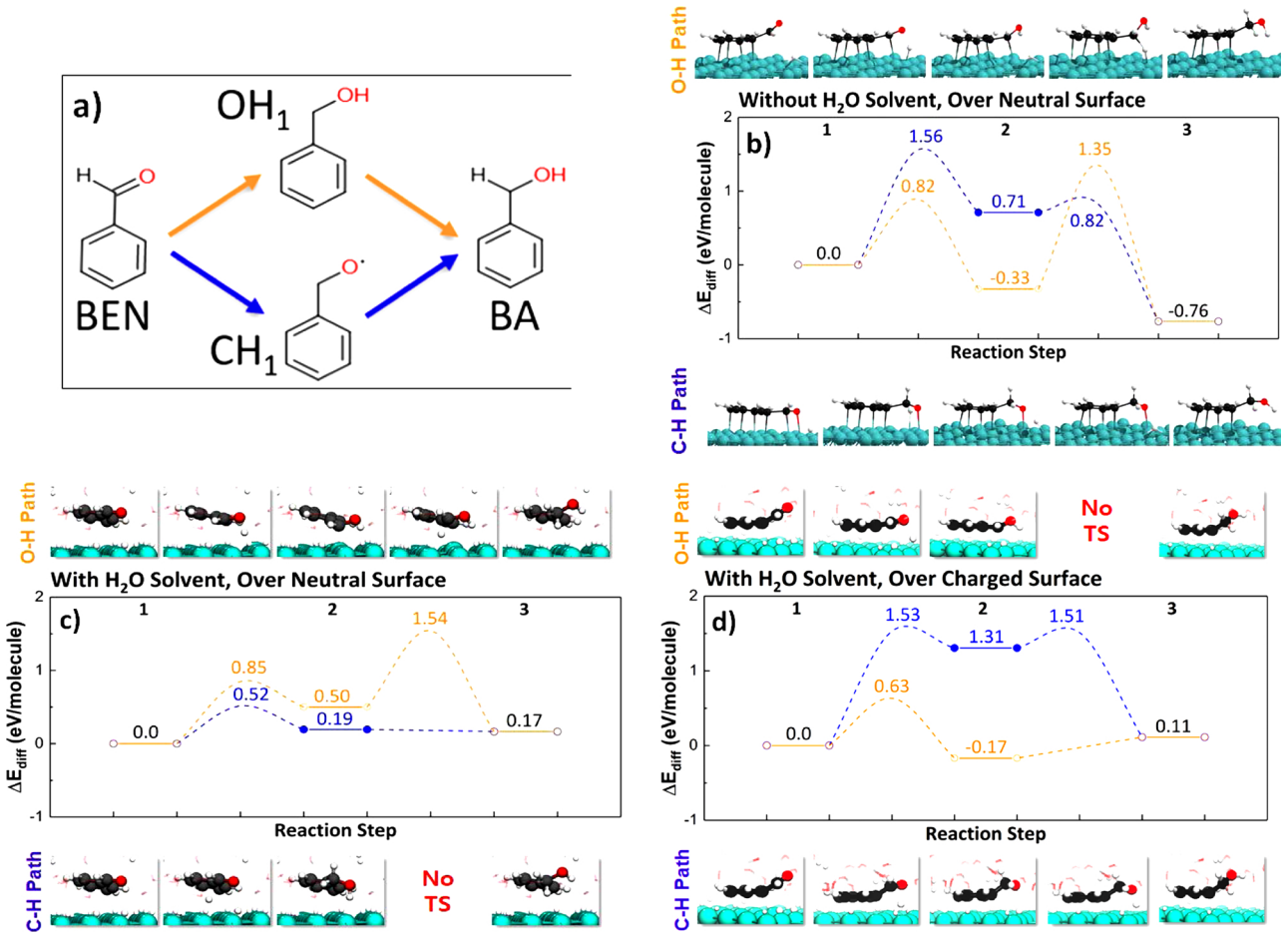


**Fig. 5.** a) Proposed Langmuir-Hinshelwood mechanism (C-H vs. O-H pathway) for benzaldehyde (BEN) hydrogenation to benzyl alcohol (BA) over Pd(111) surface, along with DFT-based reaction pathways of benzaldehyde hydrogenation b) without and c) with the presence of $H_2O$ solvent over neutral surface and d) with the presence of $H_2O$ solvent over charged surface. Note that the reference state is the adsorbed benzaldehyde on the Pd surface. Color codes for surface models: H (white), O (red), C (black) and Pd (cyan). (For interpretation of the references to colour in the Figure, the reader is referred to the web version of this article).

at the second hydrogenation step. Thus, in the gas phase, the O—H pathway should be prevalent route, similar to the case of $CO_2$ reduction over Cu(111) [51]. The potential energy landscape of benzaldehyde hydrogenation over the neutral Pd surface becomes greatly changed with the incorporation of $H_2O$ solvent (see Fig. 5c). Now, the C—H pathway become a thermodynamically and kinetically favorable route over the O-H pathway since it possesses both a more stable reaction intermediates and a lower activation barrier between the hydrogenation steps. In fact, the second hydrogenation step of C—H pathway is a spontaneous process unlike for the O—H pathway. This is the result of the fact that the intermediates in the C—H pathway is partially charged at the oxygen and therefore, stabilized by the solvent. This is consistent with the observation for keto/enol tautomerization reactions on Pt surfaces [14], indicating the important role of explicit $H_2O$ for hydrogenation processes of polar organic functional groups.

Furthermore, we also explore the case where the benzaldehyde hydrogenation now occurs on the charged Pd(111) surface (see Fig. 5d). Interestingly, even in the presence of $H_2O$ solvent, the O-H pathway now becomes a thermodynamically and kinetically preferable route over the C—H pathway on the charged surface. We observed that the intermediate of the O—H pathway is strongly stabilized by the surface charge, leading to a build-up of density on the carbonyl carbon. As a result, the second hydrogenation of O—H pathway is spontaneous. Conversely, the partially and negatively charged intermediate of C—H pathway is destabilized due to Coulombic repulsion with the negatively charged Pd surface. This also raises the barriers between hydrogenation steps. Overall, the consideration of $H_2O$ solvent and surface charge induces significant changes on the thermodynamic and kinetic aspects of benzaldehyde hydrogenation over the metal surface, but for the case of Pd(111), charge transfer to the surface-bound intermediate will substantially reduce hydrogenation barriers and lower *k*.

## 4. Conclusions

In summary, we have studied the hydrogenation reaction of benzaldehyde over the Pt(111) and Pd(111) surfaces based on a LH mechanism. The initial investigation on the surface H coverages over the Pd and Pt(111) surfaces reveals that the mixture of H adsorption site is presented on the Pt(111) while the fcc adsorption site is dominantly occupied by H atom on the Pd(111). Also, while the adsorbed benzaldehyde is titled away from the neutral Pd surface, it lies flat on the charged Pd surface in the presence of $H_2O$ solvent. More importantly, we show that the consideration of $H_2O$ solvent and surface charge is essential in understanding the thermodynamic and kinetic profiles of benzaldehyde hydrogenation over the metal surface. The stability of reaction intermediates and the activation barrier between hydrogenation steps is greatly changed in the presence of $H_2O$ solvent and surface charge on the Pd(111) surface. Critical for the current discussion is the role of charge transfer in the presence of liquid (both with and without external potentials). When charge transfer occurs from the metal to the organics, the solvent can stabilize intermediates and/or reactants, leading to the rate enhancement by increasing coverage, lowering reaction barriers particularly the proton transfer events, and introducing alternate reaction routes. The addition of electrochemical potential can

enhance the charge transfer and therefore also enhance rates.

## CRediT authorship contribution statement

**Simuck F. Yuk:** Writing - original draft, Data curation, Formal analysis. **Mal-Soon Lee:** Conceptualization, Supervision, Data curation, Formal analysis, Writing - review & editing. **Sneha A. Akhade:** Data curation, Formal analysis, Writing - review & editing. **Manh-Thuong Nguyen:** Writing - review & editing. **Vassiliki-Alexandra Glezakou:** Writing - review & editing, Funding acquisition. **Roger Rousseau:** Writing - review & editing, Funding acquisition.

## Declaration of Competing Interest

The authors report no declarations of interest.

## Acknowledgements

This work was supported by Chemical Transformation Initiative, funded by the Laboratory Directed Research and Development (LDRD) program at Pacific Northwest National Laboratory (PNNL). PNNL is operated by Battelle for the US Department of Energy under Contract DE-AC05-76RL01830. Computational Resources were provided by PNNL Research Computing. Writing of the manuscript by SAA was performed under the auspices of the US Department of Energy by Lawrence Livermore National Laboratory (LLNL) under Contract DEAC52-07NA27344.

## Appendix A. Supplementary data

Supplementary material related to this article can be found, in the online version, at doi:https://doi.org/10.1016/j.cattod.2020.07.039.

## References

[1] G.W. Huber, S. Iborra, A. Corma, Synthesis of transportation fuels from biomass: chemistry, catalysts, and engineering, Chem. Rev. 106 (2006) 4044–4098.
[2] J.C. Serrano-Ruiz, J.A. Dumesic, Catalytic routes for the conversion of biomass into liquid hydrocarbon transportation fuels, Energy Environ. Sci. 4 (2011) 83–99.
[3] R.S. Weber, J.E. Holladay, Modularized production of value-added products and fuels from distributed waste carbon-rich feedstocks, Engineering 4 (2018) 330–335.
[4] P. Vennestrøm, C.M. Osmundsen, C. Christensen, E. Taarning, Beyond petrochemicals: the renewable chemicals industry, Angew. Chem. Int. Ed. 50 (2011) 10502–10509.
[5] U.K. Singh, M.A. Vannice, Kinetics of liquid-phase hydrogenation reactions over supported metal catalysts—a review, Appl. Catal. A 213 (2001) 1–24.
[6] J.N. Chheda, G.W. Huber, J.A. Dumesic, Liquid-phase catalytic processing of biomass-derived oxygenated hydrocarbons to fuels and chemicals, Angew. Chem. Int. Ed. 46 (2007) 7164–7183.
[7] D.C. Cantu, A.B. Padmaperuma, M.-T. Nguyen, S.A. Akhade, Y. Yoon, Y.-G. Wang, M.-S. Lee, V.-A. Glezakou, R. Rousseau, M.A. Lilga, A combined experimental and theoretical study on the activity and selectivity of the electrocatalytic hydrogenation of aldehydes, ACS Catal. 8 (2018) 7645–7658.
[8] N. Singh, U. Sanyal, G. Ruehl, K.A. Stoerzinger, O.Y. Gutiérrez, D.M. Camaioni, J.L. Fulton, J.A. Lercher, C.T. Campbell, Aqueous phase catalytic and electrocatalytic hydrogenation of phenol and benzaldehyde over platinum group metals, J. Catal. 382 (2020) 372–384.
[9] K. Koh, U. Sanyal, M.S. Lee, G. Cheng, M. Song, V.A. Glezakou, Y. Liu, D. Li, R. Rousseau, O.Y. Gutiérrez, Electrochemically tunable proton-coupled electron transfer in Pd-catalyzed benzaldehyde hydrogenation, Angew. Chem. 132 (2020) 1517–1521.
[10] S.D. Lin, M.A. Vannice, Hydrogenation of aromatic hydrocarbons over supported Pt catalysts. I. Benzene hydrogenation, J. Catal. 143 (1993) 539–553.
[11] D.S. Santana, G.O. Melo, M.V. Lima, J.R. Daniel, M.C. Areias, M. Navarro, Electrocatalytic hydrogenation of organic compounds using a nickel sacrificial anode, J. Electroanal. Chem. 569 (2004) 71–78.
[12] A. Saadi, R. Merabti, Z. Rassoul, M. Bettahar, Benzaldehyde hydrogenation over supported nickel catalysts, J. Mol. Catal. A: Chem. 253 (2006) 79–85.
[13] A. Bannari, P. Proulx, H. Ménard, C.M. Cirtiu, Mathematical modeling of the kinetics of phenol electrocatalytic hydrogenation over supported Pd–alumina catalyst, Appl. Catal. A 345 (2008) 28–42.
[14] Y. Yoon, R. Rousseau, R.S. Weber, D. Mei, J.A. Lercher, First-principles study of phenol hydrogenation on Pt and Ni catalysts in aqueous phase, J. Am. Chem. Soc. 136 (2014) 10287–10298.
[15] N. Singh, Y. Song, O.Y. Gutiérrez, D.M. Camaioni, C.T. Campbell, J.A. Lercher, Electrocatalytic hydrogenation of phenol over platinum and rhodium: unexpected temperature effects resolved, ACS Catal. 6 (2016) 7466–7470.
[16] U. Sanyal, Y. Song, N. Singh, J.L. Fulton, J. Herranz, A. Jentys, O.Y. Gutiérrez, J.A. Lercher, Structure sensitivity in hydrogenation reactions on Pt/C in aqueous-phase, ChemCatChem 11 (2019) 575–582.
[17] N. Singh, M.-S. Lee, S.A. Akhade, G. Cheng, D.M. Camaioni, O.Y. Gutiérrez, V.-A. Glezakou, R. Rousseau, J.A. Lercher, C.T. Campbell, Impact of pH on aqueous-phase phenol hydrogenation catalyzed by carbon-supported Pt and Rh, ACS Catal. 9 (2018) 1120–1128.
[18] N. Singh, M.-T. Nguyen, D.C. Cantu, B.L. Mehdi, N.D. Browning, J.L. Fulton, J. Zheng, M. Balasubramanian, O.Y. Gutiérrez, V.-A. Glezakou, Carbon-supported Pt during aqueous phenol hydrogenation with and without applied electrical potential: X-ray absorption and theoretical studies of structure and adsorbates, J. Catal. 368 (2018) 8–19.
[19] J.A. Lopez-Ruiz, E. Andrews, S.A. Akhade, M.-S. Lee, K. Koh, U. Sanyal, S.F. Yuk, A.J. Karkamkar, M.A. Derewinski, J. Holladay, Understanding the role of metal and molecular structure on the electrocatalytic hydrogenation of oxygenated organic compounds, ACS Catal. 9 (2019) 9964–9972.
[20] Y. Song, U. Sanyal, D. Pangotra, J.D. Holladay, D.M. Camaioni, O.Y. Gutiérrez, J.A. Lercher, Hydrogenation of benzaldehyde via electrocatalysis and thermal catalysis on carbon-supported metals, J. Catal. 359 (2018) 68–75.
[21] M.A. Vannice, D. Poondi, The effect of metal-support interactions on the hydrogenation of benzaldehyde and benzyl alcohol, J. Catal. 169 (1997) 166–175.
[22] T.T.T. Hanh, Y. Takimoto, O. Sugino, First-principles thermodynamic description of hydrogen electroadsorption on the Pt(111) surface, Surf. Sci. 625 (2014) 104–111.
[23] A. Michaelides, P. Hu, A density functional theory study of $CH_2$ and H adsorption on Ni(111), J. Chem. Phys. 112 (2000) 6006–6014.
[24] C.D. Vurdu, The adsorption and diffusion manners of hydrogen atoms on Pt(100), Pt (110), and Pt(111) surfaces, Adv. Cond. Matter Phys. 2018 (2018) 4186968.
[25] W. Dong, V. Ledentu, P. Sautet, A. Eichler, J. Hafner, Hydrogen adsorption on palladium: a comparative theoretical study of different surfaces, Surf. Sci. 411 (1998) 123–136.
[26] P. Ferrin, S. Kandoi, A.U. Nilekar, M. Mavrikakis, Hydrogen adsorption, absorption and diffusion on and in transition metal surfaces: a DFT study, Surf. Sci. 606 (2012) 679–689.
[27] G. Yang, S.A. Akhade, X. Chen, Y. Liu, M.S. Lee, V.A. Glezakou, R. Rousseau, J.A. Lercher, The nature of hydrogen adsorption on platinum in the aqueous phase, Angew. Chem. Int. Ed. 58 (2019) 3527–3532.
[28] J.P. Perdew, K. Burke, M. Ernzerhof, Generalized gradient approximation made simple, Phys. Rev. Lett. 77 (1996) 3865.
[29] B.G. Lippert, J. Hutter, M. Parrinello, A hybrid Gaussian and plane wave density functional scheme, Mol. Phys. 92 (1997) 477–488.
[30] J. VandeVondele, M. Krack, F. Mohamed, M. Parrinello, T. Chassaing, J. Hutter, Quickstep: Fast and accurate density functional calculations using a mixed Gaussian and plane waves approach, Comput. Phys. Commun. 167 (2005) 103–128.
[31] S. Goedecker, M. Teter, J. Hutter, Separable dual-space Gaussian pseudopotentials, Phys. Rev. B 54 (1996) 1703.
[32] J. VandeVondele, J. Hutter, Gaussian basis sets for accurate calculations on molecular systems in gas and condensed phases, J. Chem. Phys. 127 (2007) 114105.
[33] S. Grimme, J. Antony, S. Ehrlich, H. Krieg, A consistent and accurate ab initio parametrization of density functional dispersion correction (DFT-D) for the 94 elements H-Pu, J. Chem. Phys. 132 (2010) 154104.
[34] Y.-N. Wen, J.-M. Zhang, Surface energy calculation of the fcc metals by using the MAEAM, Solid State Commun. 144 (2007) 163–167.
[35] N.E. Singh-Miller, N. Marzari, Surface energies, work functions, and surface relaxations of low-index metallic surfaces from first principles, Phys. Rev. B 80 (2009) 235407.
[36] A. Patra, J.E. Bates, J. Sun, J.P. Perdew, Properties of real metallic surfaces: effects of density functional semilocality and van der Waals nonlocality, Proc. Natl. Acad. Sci. 114 (2017) E9188–E9196.
[37] G. Henkelman, B.P. Uberuaga, H. Jónsson, A climbing image nudged elastic band method for finding saddle points and minimum energy paths, J. Chem. Phys. 113 (2000) 9901–9904.
[38] W. Humphrey, A. Dalke, K. Schulten, VMD: visual molecular dynamics, J. Mol. Graphics 14 (1996) 33–38.
[39] G.W. Watson, R.P. Wells, D.J. Willock, G.J. Hutchings, A comparison of the adsorption and diffusion of hydrogen on the {111} surfaces of Ni, Pd, and Pt from density functional theory calculations, J. Phys. Chem. B 105 (2001) 4889–4894.
[40] I.A. Pašti, N.M. Gavrilov, S.V. Mentus, Hydrogen adsorption on palladium and platinum overlayers: DFT study, Adv. Phys. Chem. 2011 (2011).
[41] R.I. Masel, Principles of adsorption and reaction on solid surfaces, John Wiley & Sons, Illinois, 1996.
[42] L. Delle Site, A. Alavi, C. Abrams, Adsorption energies and geometries of phenol on the (111) surface of nickel: an ab initio study, Phys. Rev. B 67 (2003) 193406.
[43] L.M. Ghiringhelli, R. Caputo, L. Delle Site, Phenol near Ni(111), Ni(110), and Ni (221) surfaces in a vertical ring geometry: A density functional study of the oxygen-surface bonding and OH cleavage, Phys. Rev. B 75 (2007) 113403.
[44] A.M. Rasmussen, B. Hammer, Adsorption, mobility, and dimerization of benzaldehyde on Pt(111), J. Chem. Phys. 136 (2012) 174706.
[45] M.-T. Nguyen, S.A. Akhade, D.C. Cantu, M.-S. Lee, V.-A. Glezakou, R. Rousseau, Electro-reduction of organics on metal cathodes: A multiscale-modeling study of benzaldehyde on Au(111), Catal. Today (2019).
[46] N. Singh, C.T. Campbell, A simple bond-additivity model explains large decreases in heats of adsorption in solvents versus gas phase: a case study with phenol on Pt (111) in water, ACS Catal. 9 (2019) 8116–8127.
[47] D.C. Cantu, Y.-G. Wang, Y. Yoon, V.-A. Glezakou, R. Rousseau, R.S. Weber,

Heterogeneous catalysis in complex, condensed reaction media, Catal. Today 289 (2017) 231–236.
[48] J.O.M. Bockris, K.T. Jeng, In-situ studies of adsorption of organic compounds on platinum electrodes, J. Electroanal. Chem. 330 (1992) 541–581.
[49] J.A. Lopez-Ruiz, U. Sanyal, J. Egbert, O.Y. Gutiérrez, J. Holladay, Kinetic investigation of the sustainable electrocatalytic hydrogenation of benzaldehyde on Pd/C: Effect of electrolyte composition and half-cell potentials, ACS Sustain. Chem. Eng. 6 (2018) 16073–16085.
[50] S.A. Akhade, W. Luo, X. Nie, A. Asthagiri, M.J. Janik, Theoretical insight on reactivity trends in $CO_2$ electroreduction across transition metals, Catal. Sci 6 (2016) 1042–1053.
[51] X. Nie, M.R. Esopi, M.J. Janik, A. Asthagiri, Selectivity of $CO_2$ reduction on copper electrodes: the role of the kinetics of elementary steps, Angew. Chem. Int. Ed. 52 (2013) 2459–2462.